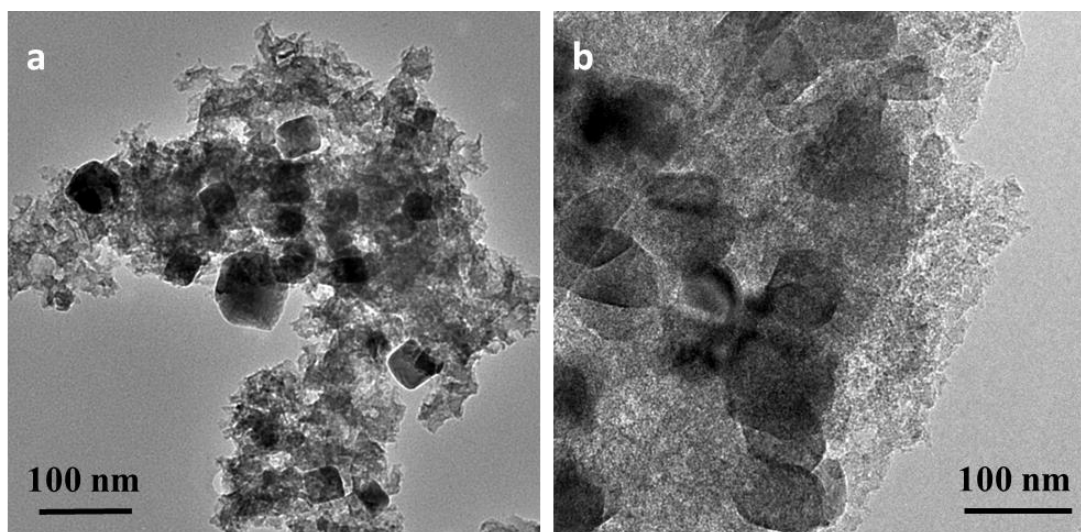


***In-situ* preparation of  $\text{Ca}_{0.5}\text{Mn}_{0.5}\text{O/C}$  as a novel high-activity catalyst for oxygen reduction reaction**

Yu-Qi Lyu, Chi Chen, Yang Gao, Mattia Saccoccio, and Francesco Ciucci\*

## 1. Physical characterization



**Figure S1.** TEM image of (a) MnO/C and (b) Ca<sub>0.5</sub>Mn<sub>0.5</sub>O/C

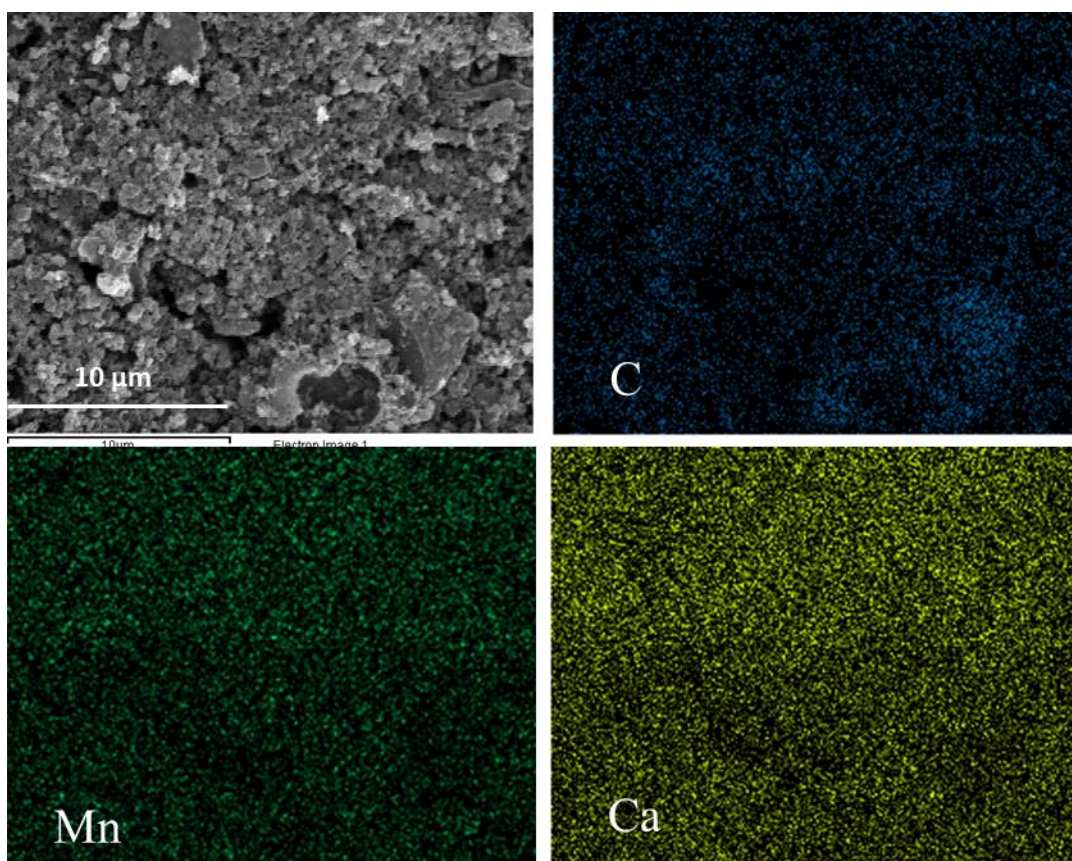


**Figure S2.** SEM image and EDS mapping of Ca<sub>0.5</sub>Mn<sub>0.5</sub>O/C. From the EDS mapping, one can see that C, Mn, and Ca are evenly distributed, which suggests that the Ca-substitution is uniform over the whole material.

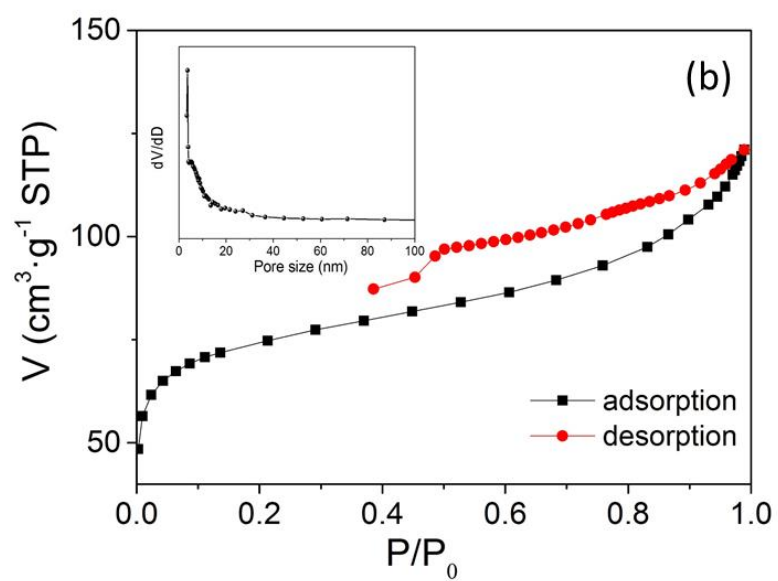


**Figure S3.** N<sub>2</sub> adsorption-desorption isotherms of MnO/C.

## 2. Activity per material cost

**Table S1.** Market price of Pt, Mn, and Ca<sup>1</sup>

	Price (\$/kg <sup>-1</sup> )	Annual production (kg)
Pt	$5.01 \times 10^4$	$1.99 \times 10^5$
Mn	3.98	$1.26 \times 10^{10}$
Ca	-	$>3.16 \times 10^{10}$

### 3. Thermogravimetric analysis (TGA)

The composition of two materials is also studied by TGA, as shown in Figure S4. The two catalysts were dried at 200 °C for 2 h before measurement. After oxidation to 900 °C at the rate of 5 °C/s in dry air, the remaining weight is 42.8 % and 38.16 % for  $\text{Ca}_{0.5}\text{Mn}_{0.5}\text{O}/\text{C}$  and  $\text{MnO}/\text{C}$ , respectively. This means that  $\text{Ca}_{0.5}\text{Mn}_{0.5}\text{O}$  and  $\text{MnO}$  account for 42.8 % and 38.16 % of the total masses of the respective composites. This result is in good agreement with the mass concentration of the metals obtained from ICP. In addition, the weight losses represent the mass content of carbon and both values are similar for both materials (57.2 % for  $\text{Ca}_{0.5}\text{Mn}_{0.5}\text{O}/\text{C}$  and 61.84 % for  $\text{MnO}/\text{C}$ ).

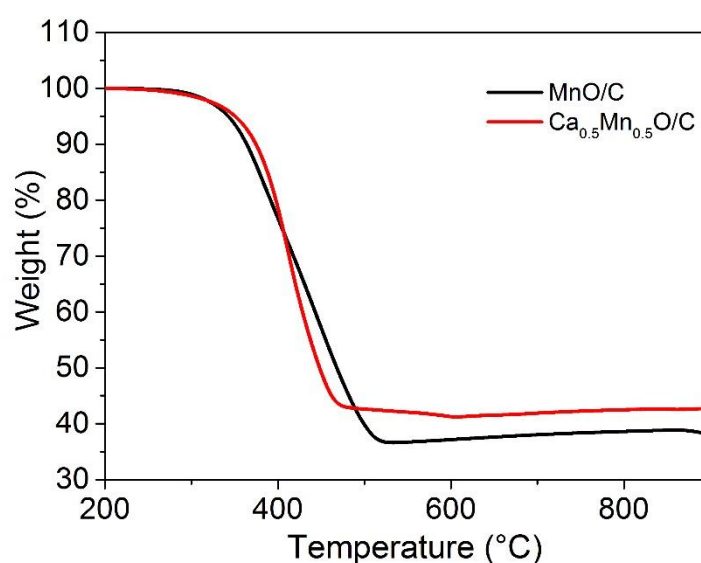


**Figure S4.** TGA curve obtained for  $\text{Ca}_{0.5}\text{Mn}_{0.5}\text{O}/\text{C}$  and  $\text{MnO}/\text{C}$  in air.

#### 4. ORR performance evaluation of MnO/C

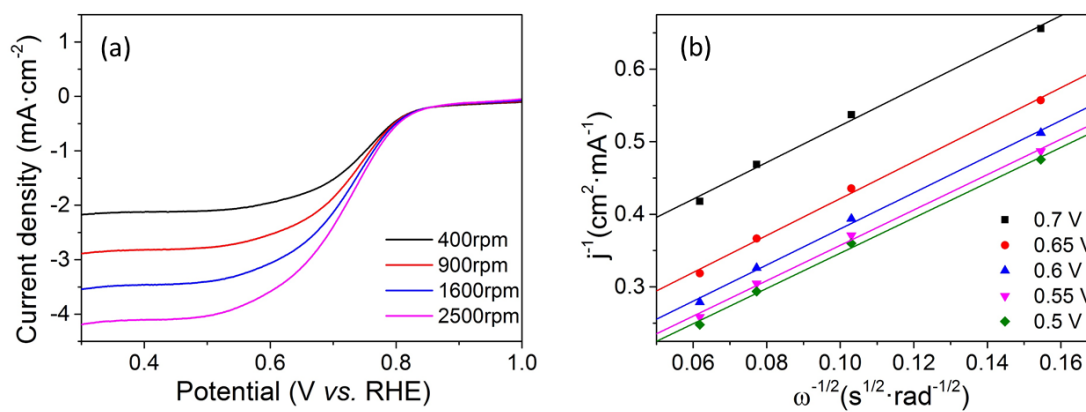


**Figure S5.** (a) LSV curves of MnO/C at the rotation speed from 400 rpm to 1600 rpm, and (b) the corresponding Koutechy-Levich plots.

## 5. Structural study of pristine $\text{Ca}_{0.5}\text{Mn}_{0.5}\text{O}$

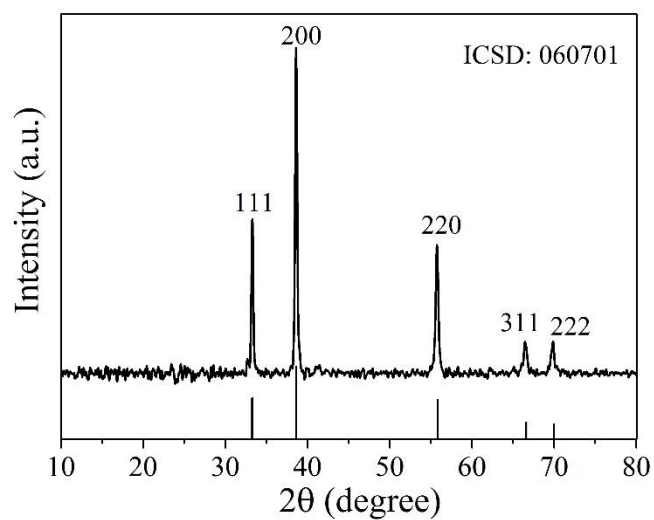


**Figure S6.** The XRD pattern of the pristine  $\text{Ca}_{0.5}\text{Mn}_{0.5}\text{O}$

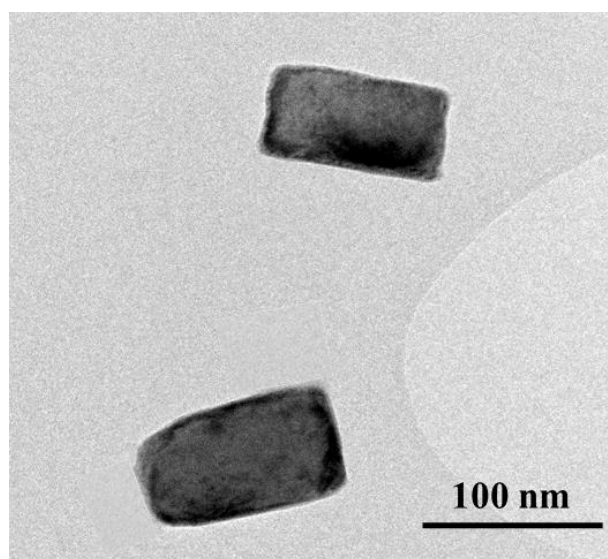


**Figure S7.** The TEM image of the pristine  $\text{Ca}_{0.5}\text{Mn}_{0.5}\text{O}$

## 6. Ca 2p XPS spectrum of $\text{Ca}_{0.5}\text{Mn}_{0.5}\text{O}/\text{C}$

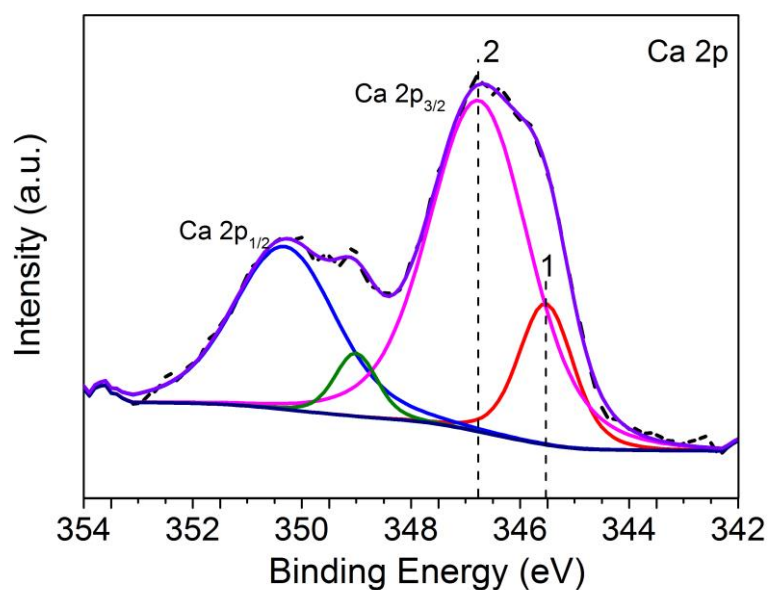


**Figure S8.** Ca 2p XPS spectrum of  $\text{Ca}_{0.5}\text{Mn}_{0.5}\text{O}/\text{C}$ . Both Ca 2p<sub>1/2</sub> and Ca 2p<sub>3/2</sub> can be deconvoluted into two peaks. The binding energy (BE) at around 345.5 eV (peak 1) and 346.5 eV (peak 2) were assigned to Ca-O and Ca-OH species<sup>2</sup>, respectively. The area of peak 2 is relatively larger than that of peak 1, which, in conjunction with O 1s spectrum, suggests that the outermost surface of  $\text{Ca}_{0.5}\text{Mn}_{0.5}\text{O}$  is covered by OH groups in a large extent.

## References

1. Vesborg, P. C.; Jaramillo, T. F., Addressing the terawatt challenge: scalability in the supply of chemical elements for renewable energy. *RSC Advances* **2012**, *2* (21), 7933-7947.
2. Granados, M. L.; Poves, M. Z.; Alonso, D. M.; Mariscal, R.; Galisteo, F. C.; Moreno-Tost, R.; Santamaría, J.; Fierro, J., Biodiesel from sunflower oil by using activated calcium oxide. *Applied Catalysis B: Environmental* **2007**, *73* (3), 317-326.